Organic Electronics 13 (2012) 409–418

Contents lists available at SciVerse ScienceDirect

Organic Electronics

journal homepage: www.elsevier.com/locate/orgel

A comparative assessment of surface microstructure and electrical conductivity dependence on co-solvent addition in spin coated and inkjet printed poly(3,4-ethylenedioxythiophene):polystyrene sulphonate (PEDOT:PSS)

Peter Wilson, Constantina Lekakou *, John F. Watts

Division of Mechanical, Medical, and Aerospace Engineering, Faculty of Engineering and Physical Sciences, University of Surrey, Guildford GU2 7XH, UK

ARTICLE INFO

Article history:
Received 9 June 2011
Received in revised form 9 November 2011
Accepted 19 November 2011
Available online 15 December 2011

Keywords:
Inkjet printing
Spin coating
PEDOT:PSS
AFM
XPS
Electrical conductivity

ABSTRACT

This study focuses on the fabrication of poly(3,4-ethylenedioxythiophene):polystyrene sulphonate (PEDOT:PSS) thin films by inkjet printing and investigates the developed surface morphology and electrical conductivity of the printed films as a function of the concentration of dimethyl sulfoxide (DMSO), added as conduction enhancing co-solvent, and Surfynol, added as a surfactant. The printed films are compared with PEDOT:PSS films fabricated by the traditional spin coating technique. Measurements of the surface tension justify including surfactant as a processing additive, where addition of 1% Surfynol results in substantial decrease of the surface tension of the PEDOT:PSS solution, whilst it also increases film surface roughness by an order of magnitude for both fabrication methods. The addition of 5 wt% DMSO is shown to result in a 10^3 decrease in sheet resistance for both spin coated and inkjet printed films with both processing routes demonstrating decrease in surface roughness and coarsening of PEDOT grains as a function of the co-solvent concentration, whilst X-ray photon spectroscopy showed an increase in the surface PEDOT to PSS ratio from 0.4 to 0.5. Inkjet printed films have lower sheet resistance than the corresponding spin coated films, whilst atomic force microscopy reveals a coarser surface morphology for the inkjet printed films. The findings in this work point out at the decrease of sheet resistance due to coarsening of PEDOT grains which is linked to a decrease of surface roughness for small RMS values associated with the PEDOT grains. However, the higher surface roughness generated when Surfynol surfactant was added was not detrimental to the film's in-plane conductivity due to the fact that these higher roughness values were unrelated to the PEDOT grains.

1. Introduction

The introduction of organic electronics has seen a torrent of research into thin film plastic devices. The potential for increased flexibility, performance and cost effectiveness over the more common inorganic materials has generated much interest in the fields of light emitters [1–3], high volume photovoltaics [4–8] and RF antennae [9,10] all of which can take advantage of the new properties and production methods open to plastic electronics. Indeed, solution coating, in the form of spin coating, gravure/doctor blade and inkjet printing have themselves opened up new areas for research with a number of devices showing performance related to the processing method of choice [11–13].

Central to the work of a number of groups is the highly conducting PEDOT:PSS polymer whose exceptional conductivity, 570 S/cm [14], high flexibility and thermal

* Corresponding author. Tel.: +44 (0) 14 83 68 9622; fax: +44 (0) 14 83 68 6291.
E-mail address: C.Lekakou@surrey.ac.uk (C. Lekakou).

1566-1199/$ - see front matter © 2011 Elsevier B.V. All rights reserved.
doi:10.1016/j.orgel.2011.11.011

stability have demonstrated exceptional value as a high work function anode in OLEDs [15], photovoltaic cells [16] and as the source/drain electrodes in thin film transistors [17]. Whilst the beneficial electrical properties of PEDOT:PSS such as high work function, hole transporting and electron blocking properties, and tuneable bandgap have been documented, a number of groups have reasoned that the marked improvement in the lifetime of a device can be attributed to the improved surface properties of spin cast PEDOT:PSS over more conventional transparent anodes such as ITO [18]. Despite the performance of PEDOT:PSS, spin coating, which remains the defacto method for rapid prototyping of thin film deposition, offers little potential for mass production due to the excessive waste and the inability to pattern precise, intricate shapes [19].

With many decades of development, inkjet printing has proven itself as the industry standard for small/medium volume, high intricacy, repeatable solution patterning. With single specialist jetters capable of providing orifice diameters down to 30 μm, droplet sizes a fraction of this are possible through the negative/positive 'Purdue', wave architecture [20,21] in the case of piezoelectrically driven units. Conversely, with drop ejection rates of 10^5 s^{-1} large areas can be patterned quickly without losing the capability for shape complexity. Furthermore, by tailoring solution concentration, including additives, such as surfactants and humectants, and altering processing conditions, including substrate temperature or atmosphere, complex 3D patterning can be achieved through multiple and interfacial layering.

It has been widely acknowledged that the inclusion of a high boiling point co-solvent, such as sorbitol or dimethyl sulfoxide, can have a dramatic effect on the conductivity of the PEDOT:PSS layer [22]. Fig. 1 displays a schematic representation of the PEDOT:PSS which illustrates the hole conducting PEDOT chain and an adjacent PSS chain, where PSS generally surrounds PEDOT to form a PEDOT nano-dispersion in water and it also provides a counter polyanion chain to the positively charged PEDOT during hole conduction. Several authors [23–25] have reported conductivity increases of the order of 10^3 when a solvent is added compared to pristine PEDOT:PSS layers, yet the relationship between surface properties and conductivity needs further investigation. In a series of papers [24–27], Nardes et al. attributed this in-plane conductivity increase in spin coated films to the in-plane decrease of the non conducting PSS interface between conducting PEDOT grains when Sorbitol solvent was added [24]. However, this has not been verified with a wide range of studies, including different processing conditions or comparing different processing techniques.

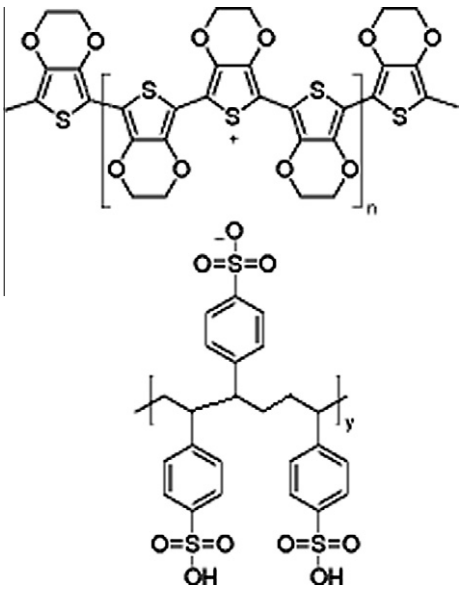

Fig. 1. Schematic representation of poly(3,4-ethylenedioxythiophene)–poly(styrenesulfonate) (PEDOT:PSS).

Additionally non-specialist inkjet units have a very narrow band of acceptable fluid rheology; for example, Epson piezoelectric ink heads require fluids with viscosity in the range of 2–6 mPa s and surface tension of the order of 30–34 mN m^{-1}. Common household inkjet inks contain a range of additives beyond the co-solvent and dye solution. Water-miscible organic co-solvents control the wetting and drying characteristics, binders ensure the dye adheres to the substrate whilst humectants prevent crusting at the nozzle. Additionally, surfactants control spreading and biocides repress biological growth. Furthermore, defoamers, anti-cockle and pH controllers are also added.

This paper will investigate the effects of two such additives, a co-solvent and a surfactant, on the electrical and surface properties of PEDOT:PSS thin films fabricated by two alternative processing techniques: inkjet printing and spin coating. In this study, a range of PEDOT:PSS solutions have been characterised in terms of their surface tension and the electrical conductivity of their thin films. The effect of substrate temperature on the profile of the printed drop was investigated to optimise printed patterns. Finally, each sample was analysed via atomic force microscopy (AFM) to gain an understanding of the surface morphology and its dependence on processing technique, co-solvent and surfactant, while the surface morphology was also related to surface conductivity in order to optimise the composition of the feed solution and to compare the inkjet printing technique to spin coating.

2. Experimental

Conductive grade PEDOT:PSS (1.3 wt% in water, σ = 1 S/cm; from Sigma–Aldrich) was used as the starting solution. Laboratory reagent grade dimethyl sulfoxide (DMSO) (from Sigma–Aldrich) was used as co-solvent. Surfynol 2502 (from AirProducts) was used as non-foaming surfactant. Surface tension of the solutions was measured on a Kruss EasyDrop DSA15 drop analyser at room temperature using the sessile drop technique. The PEDOT:PSS thin films were deposited by two methods: inkjet printing and spin coating.

Primarily, films were printed onto cleaned microslide glass substrates by a custom made inkjet printing unit. The system incorporated an MJ-AT injector from MicroFab with a JetDrive III control server. The substrate was motioned via a two axis CNC controlled stage, feeding back

to the JetDrive controller. A custom G-Code compiler, written in VB Script, allowed input of the desired variables with geometry and velocity calculated thereafter. Prior scanning electron microscopy (Hitachi 3200 SEM) and profilometry analysis (Veeco Instruments Dektak 8 stylus profilometer) of the deposited drops demonstrated that the final radius of the printed droplet was approximately equal to the dispensing device orifice diameter ±20%, depending on substrate temperature. Each sample was printed at 40 Hz at a substrate temperature of 312 K to reduce line-by-line bleeding yet minimise the effect of an evaporation-rate disparity inducing redistributive flow within the drop [28,29], which was studied via profilometry for different substrate temperatures. Overlap of the drops in both X and Y position was kept at 20% whilst the dispensing velocity was maintained at ~1.5 m/s by modifying the drive wave architecture for each new set of rheological properties. The distance from the nozzle to the substrate was kept at 2 mm.

Spin coating was carried out at 3000 rpm, starting by injecting a constant volume of 3.8 ml of PEDOT:PSS solution (with the appropriate additives, depending on the specific experiment) at the centre of the spin coater and letting the volume spread on the surface via the spinning action for 30 s.

For both deposition methods 12 types of samples were prepared ranging from 0 to 5 wt% DMSO and with 0 or 1 wt% Surfynol with each solution being mixed thoroughly by an ultrasonicator and being left to stand for 24 h. 25 nm thick chromium electrodes were sputter-coated on top of the printed sample at a constant distance between the chromium electrodes to define a 2 mm^2 PEDOT:PSS film analysis area and minimise contact resistance between PEDOT:PSS and the outer electrode. Electrical measurements were conducted by taking IV curves of the samples with the gradient representing the resistance of the material, this was performed on a 2-point Ametek, Princeton Applied Research, 'VersaSTAT MC' twin channel potentiostat/galvanostat. 4-point Hall probe analysis using an Accent HL5500 Hall System was used to verify the 2-point readings. No significant disparity between the two systems was noted, as also demonstrated in [25,26].

AFM analysis was carried out using a VEECO (Digital Instruments) Nanoscope IIIa 'Multimode' Atomic Force Microscope. Each sample was analysed in tapping mode using Silicon cantilevers with an average resonant frequency of the order of 270 kHz.

XPS analysis was performed on a ThermoFisher Scientific (East Grinstead, UK) Theta Probe spectrometer. XPS spectra were acquired using a monochromated Al Kα X-ray source ($h\nu$ = 1486.6 eV). An X-ray spot of ~400 μm radius was employed. Survey spectra were acquired employing a pass energy of 300 eV. High resolution, core level spectra for C1s and O1s were acquired with a pass energy of 50 eV. All other high resolution core level spectra were acquired with a pass energy of 80 eV. All spectra were charge referenced against the C1s peak at 285 eV to correct for charging effects during acquisition. Quantitative surface chemical analysis was performed based on the high resolution, core level spectra following the removal of a non-linear (Shirley) background. The manufacturer's Avantage software was used which incorporates the appropriate sensitivity factors and corrects for the electron energy analyser transmission function.

3. Results and discussion

3.1. Drop characterisation and film optimisation in inkjet printing

The MicroFab MJ-AT dispensing device used in this investigation has a maximum permissible surface tension envelope of 70 mN m^{-1} and can print solutions of viscosity up to 20 mPa s, a notable increase over off-the-shelf units. The surface tension of the solution including a surfactant can be described by the Langmuir–Szyszkowski equation

$$\gamma(c) = \gamma_0 - \Gamma_m RT \ln(1 + K_1 c) \quad (1)$$

where γ_0 and $\gamma(c)$ denote the surface tension of the liquid free of surfactant and the surface tension as a function of surfactant concentration, respectively, Γ_m denotes a term representing the maximum amount of surfactant that can be accommodated at the interface, R represents the universal gas constant and T the temperature in Kelvin whilst K_1 is the Langmuir adsorption constant [30]. The surface tension was measured as a function of the concentration of the co-solvent DMSO for two types of PEDOT:PSS solutions without and with 1 wt% surfactant Surfynol 2502. It was found that increasing the concentration of DMSO increases the surface tension in both types of solutions although it is more pronounced in samples without surfactant in which the surface tension increases from 0.06 N/m without DMSO to 0.07 N/m for 5 wt% DMSO. The addition of Surfynol more than halves the surface tension of the solution and can accommodate large concentrations of DMSO while keeping the surface tension low. As mentioned earlier, the maximum surface tension permissible to the MicroFab jetter is reached at DMSO concentrations of 5 wt%, hence, whilst surfactants are not necessarily required for this investigation, they would be needed for printing using off-the-shelf and even some specialist inkjet printing equipment [19].

Drop size and shape in response to substrate temperature were recorded by profiling single drops in three dimensions using a Veeco Dastek 8 profilometer. Substrate temperature is selected as a compromise between quick drying times to minimise line-by-line interaction and acceptable drop profiles as demonstrated in Fig. 2. Two effects can be concluded from Fig. 2: at higher substrate temperatures the increased evaporation rate from the vapour/liquid/substrate interface generates an internal flow within the drop towards the periphery in an attempt to compensate for the increased liquid lost. The flow brings with it dissolved solute and hence redistributes it towards the outer circumference, this process is known as the "coffee cup ring effect" [31]. Secondly, one can notice a drop diameter receding proportionally to the substrate temperature as is demonstrated in Fig. 3. It is interesting to observe in Fig. 3 that whilst a small 10 K increase in substrate temperature over solution temperature results in a modest 10% decrease in the dried drop diameter, the

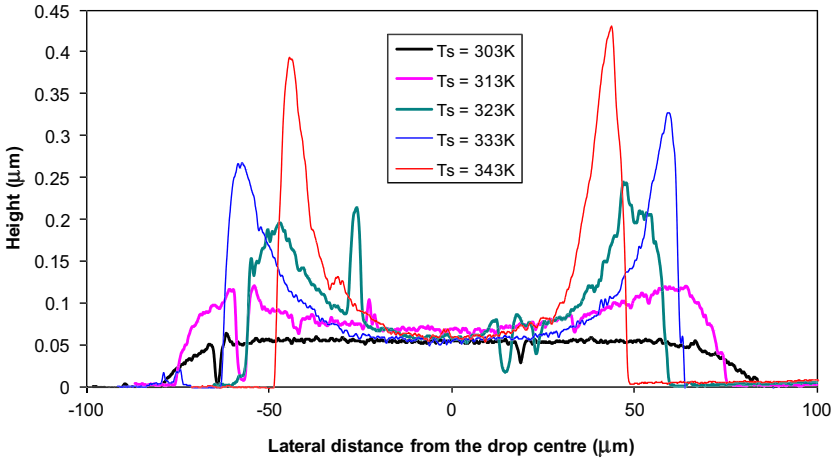

Fig. 2. Profiles of final dried printed drop shape as a function of substrate temperature.

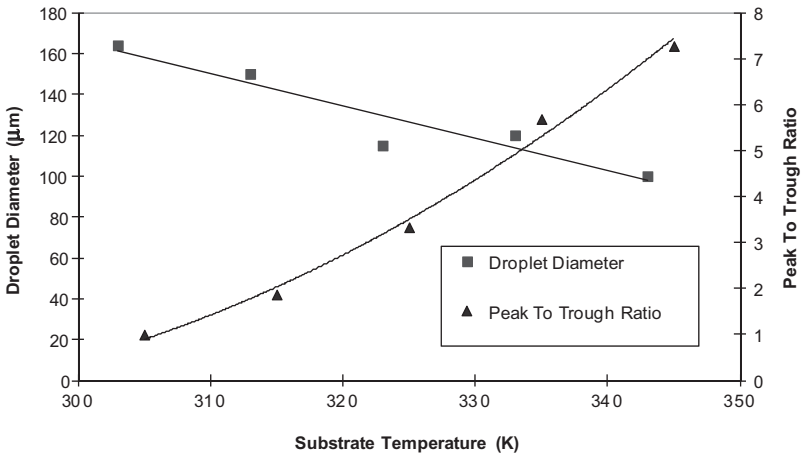

Fig. 3. Peak to trough ratio and droplet diameter as a function of substrate temperature, where the temperature of the in-flight drop was equal to the ambient temperature (298 K).

peak to trough ratio increases by a factor of 2. Whilst this process is undesirable within the context of the current investigation, it may prove useful to applications requiring high surface area interfaces.

3.2. Sheet resistance measurements

Fig. 4 displays the results of sheet resistance of the fabricated films using two alternative fabrication techniques, inkjet printing and spin coating, and feed PEDOT:PSS solutions without and with 1 wt% Surfynol surfactant and different concentrations of DMSO. As expected, the inclusion of dimethyl sulfoxide (DMSO) has a dramatic effect on the sheet resistance of both spin coated and inkjet printed thin films, with or without the addition of surfactant. The inclusion of DMSO generates a $\sim 10^3$ increase in conductivity at just 5 wt% concentration in all samples, falling from 10^7 to 10^3 Ω/□ in the case of inkjet printed samples without any surfactant, for example, as is presented in Fig. 4.

Charge transport in PEDOT:PSS occurs via Motts variable range hopping between high PEDOT concentration grains through the less conducting PSS interface [27,32]:

$$\sigma = \sigma_0 \exp\left[-\left(\frac{T_0}{T}\right)^{\gamma}\right] \tag{2}$$

where σ represents the conductivity at a temperature T, and $\gamma = \frac{1}{1+m}$ where m is the hopping dimensionality.

The addition of co-solvent is known to interfere with the PEDOT to PSS attraction resulting in a decreased PEDOT grain-to-grain distance and hence a greater charge hopping probability, according to the relation:

$$P_{ij} \propto \exp\left\{\frac{-2L}{\xi} - \frac{\Delta E_{ij}}{k_b T}\right\} \tag{3}$$

where the probability of a hop from i to j, P_{ij}, is proportional to the exponent of the characteristic hopping length, L, the localisation length, ξ, and the energy difference between states, ΔE_{ij}.

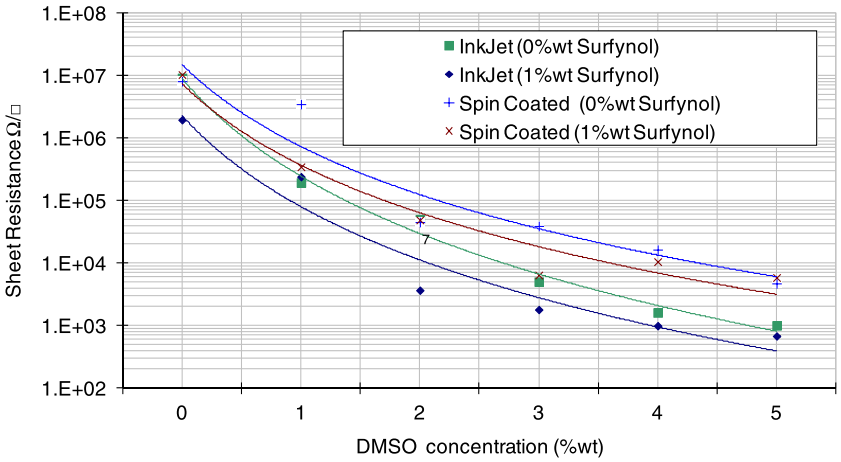

Fig. 4. Sheet resistance for inkjet printed and spin coated PEDOT:PSS thin films as a function of dimethyl sulfoxide and Surfynol surfactant concentration (sheet resistance values ±3% variation within the same sample and sheet resistance values ±20% maximum relative standard error between samples for a series of measurements of 10 different samples from each category).

It is interesting to note that the introduction of surfactant has little bearing on the sheet resistance, when compared to the effect of co-solvent, in either inkjet or spin coated films and, whilst in spin coating the surfactant ultimately has a small detrimental effect, the reverse occurs for inkjet printed films.

It is remarkable that the sheet resistance of the inkjet printed films is generally lower that the sheet resistance of the corresponding spin coated films; this effect is going to be further investigated and related to the surface morphology of the fabricated films.

3.3. Atomic force microscopy (AFM) analysis

Inkjet printed samples of different compositions in the range of 0–5 wt% DMSO and 0–1 wt% Surfynol were compared to spin coated films of corresponding compositions in AFM characterisation studies. AFM topography maps of like-for-like spin coated PEDOT:PSS films with and without surfactant are displayed in Fig. 5 whilst corresponding inkjet printed films are shown in Fig. 6. It is evident that the surfactant Surfynol 2502 creates micro-wide features at the film surface of the order of 100 nm height in both spin coated and inkjet printed films with evidence of orientation and directionality in the case of the inkjet printed film.

The effect of co-solvent DMSO can be seen better in the films with 0% Surfynol: the increase of DMSO concentration from 1 to 5 wt% leads to the coarsening of grains, suspected to be PEDOT, in both spin coated (Fig. 5a and c) and inkjet printed films (Fig. 6a and c). Fig. 7 displays the average lateral grain size in the AFM maps of inkjet printed films as the DMSO concentration is changed from 1 to 5 wt%: in general, the data confirm the PEDOT grain coarsening phenomenon as DMSO is increased from 2 to 5 wt%, while the trend is less clear for 1–2% DMSO due to the sensitivity of the measurement affecting the data at such small grain sizes. On the other hand, Fig. 8 shows that the RMS roughness of films generally decreases as DMSO concentration is increased, which seems consistent with the corresponding increase in the lateral grain size for the films with 0% Surfynol. The coarsening of PEDOT grains is expected, as increasing the amount of DMSO disrupts the PEDOT–PSS interaction, thins and ultimately erodes the PSS layer surrounding the PEDOT grains, leading to the coarsening of the PEDOT grains with obvious random patches of PSS between PEDOT grains evident at 5 wt% DMSO in Figs. 5c and 6c. This PEDOT grain coarsening effect then causes the decrease of sheet resistance of PEDOT:PSS films (Fig. 4) as the amount of added DMSO is increased. Furthermore, it is clear in Figs. 5 and 6 that the inkjet printed films have coarser PEDOT grain structure than the corresponding spin coated films, justifying the lower sheet resistance of the former (Fig. 4) due to the fact that the larger PEDOT grains provide larger regions for uninterrupted charge mobility without the charges having to hop very frequently over the insulating PSS shells.

Roughness was measured via atomic force microscopy (AFM) over 5 × 5 μm samples for all compositions, where Figs. 5 and 6 present the AFM topography maps and Fig. 8 displays the RMS roughness as a function of DMSO concentration for each type of film. Fig. 8 shows that both inkjet and spin coated fabricated films demonstrated about a 10-fold increase in roughness when containing 1 wt% Surfynol in comparison to non-surfactant containing films, 23 nm compared to 2 nm RMS roughness for inkjet printed samples with 1/0 wt% Surfynol, respectively, and 0% DMSO concentration. Both inkjet and spin coated samples demonstrated decreasing RMS roughness as a function of increasing DMSO wt%, with spin coated films (1% Surfynol) showing a shift from 27 to 10 nm RMS roughness when moving from 0 wt% DMSO to 5 wt% DMSO respectively, whilst inkjet printed samples showed a corresponding RMS roughness decrease from 23 to 18 nm. Fig. 8 demonstrates the smoothing effect the co-solvent has for both inkjet and spin coated samples. Interestingly, whilst both spin coated and inkjet printed samples show the same trend, spin coated samples with 1 wt% Surfynol surfactant demonstrate a much larger dependence on DMSO concentration than the corresponding inkjet samples, with RMS roughness in the range of 27–13 nm compared with

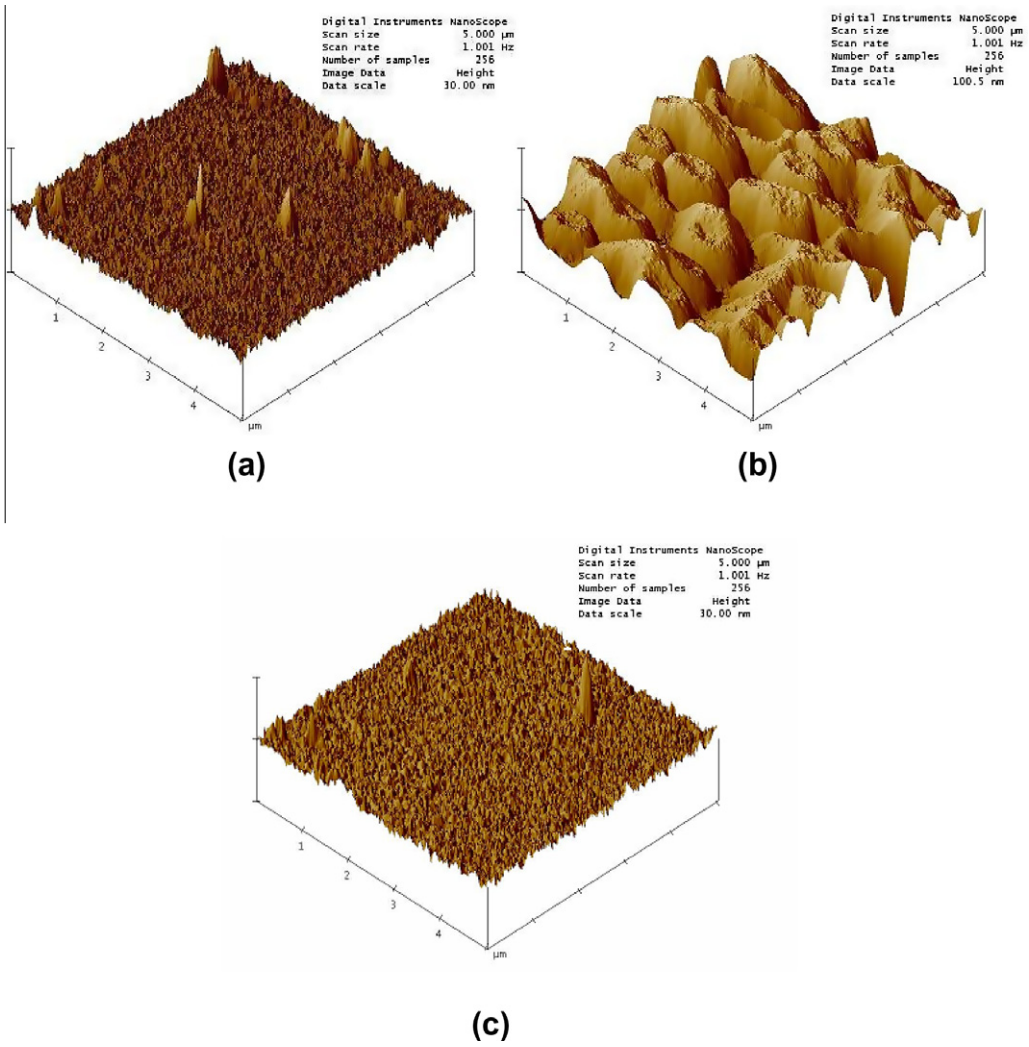

Fig. 5. 5 × 5 µm Topographical atomic force microscopy maps demonstrating spin coated PEDOT:PSS films: (a) [1 wt% DMSO/0 wt% Surfynol], (b) [1 wt% DMSO/1 wt% Surfynol], (c) [5 wt% DMSO/0 wt% Surfynol]. Data height scales are 30 nm for (a) and (c) and 100 nm for (b).

24–18 nm respectively, a 50% compared with 24% decrease in RMS roughness, respectively. However, the addition of 1 wt% Surfynol surfactant, while causing the formation of wide micro-features that increase the RMS roughness value, does not disrupt the PEDOT:PSS interactions and does not affect PEDOT grain size. As conductivity is affected by the PEDOT grain size, since the charge transport continuity in a grain is interrupted by the insulating PSS shell, the Surfynol induced micro-features do not disadvantage the film conductivity.

3.4. X-ray photon spectroscopy (XPS) analysis

The surface PEDOT to PSS ratio was studied through XPS on a range of samples whose conductivity enhancing DMSO co-solvent concentration varied between 0 and 5 wt%. XPS spectra focused on the sulphur 2p (S2p) peaks (example in insert figure in Fig. 9), with the S2p peak centralised at 164 eV representing the sulphur atom in the thiophenes of the PEDOT chain and the S2p peak centralised at 169 eV representing the sulphur atom in the sulphonate counter-ions of the PSS chain [33].

Fig. 9 shows the linear approximated dependence of surface PEDOT to PSS ratio on the DMSO concentration, where the surface PEDOT to PSS ratio increases as more DMSO is added. The results in Fig. 9 can be considered in conjunction with the coarsening of the grains in the AFM graphs of Figs. 5 and 6 and the plot in Fig. 7 when the DMSO co-solvent was increased from 1 to 5 wt%, supporting the statement that these are PEDOT grains the relative content of which seems to increase both in the coarsening effect and in the PEDOT to PSS ratio of the respective S2p peaks in the XPS analysis demonstrated in Fig. 9. Work by Kim and Ashizawa [32,34] demonstrated the effects of a solvent on the conduction mechanism, stating that the high dielectric constant of the co-solvent induces a screening effect in the electrostatic interaction between the PEDOT polymer and the counter-ion containing PSS, resulting in reducing the thickness of the PSS ‘shell’ and, hence, increase both the PEDOT to PSS ratio at the surface and the

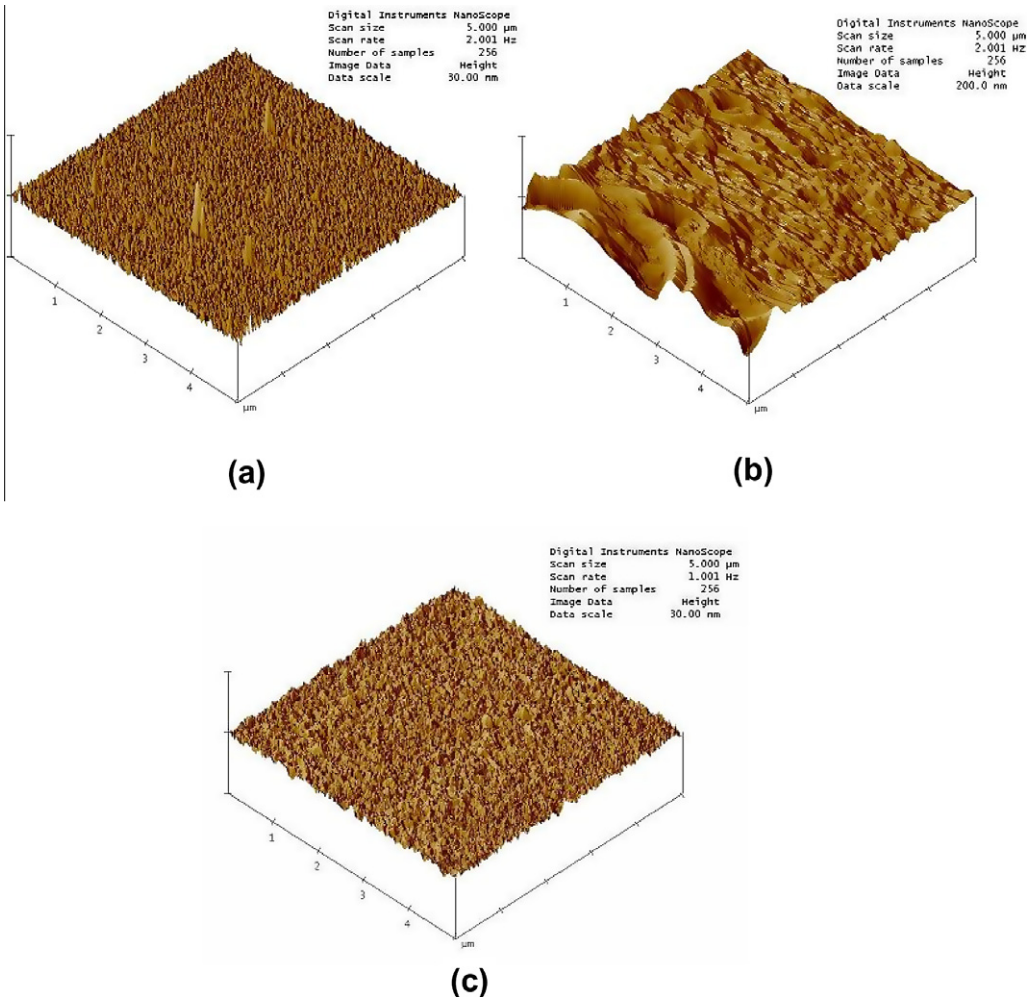

Fig. 6. 5 × 5 µm Topographical atomic force microscopy maps demonstrating inkjet printed PEDOT:PSS films: (a) [1 wt% DMSO/0 wt% Surfynol], (b) [1 wt% DMSO/1 wt% Surfynol], (c) [5 wt% DMSO/0 wt% Surfynol]. Data height scales are 30 nm for (a) and (c) and 200 nm for (b).

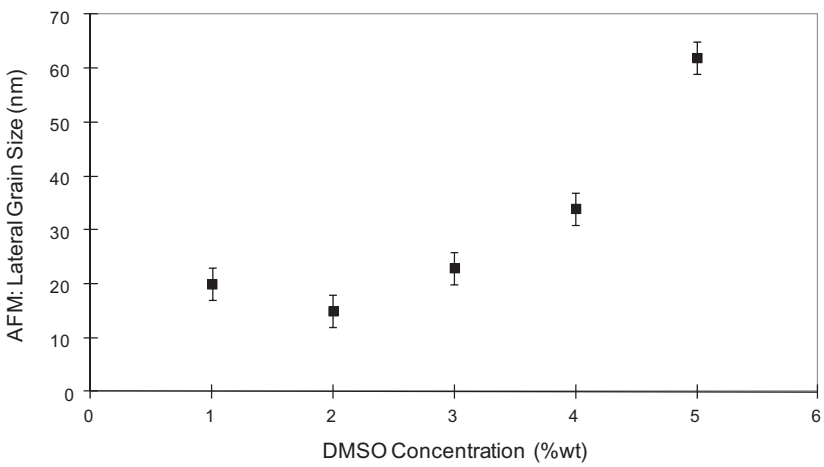

Fig. 7. Inkjet printed films: average lateral grain size in AFM micrographs (±10% maximum error in samples with 100–150 grains) as a function of dimethyl sulfoxide wt% concentration (0 wt% surfactant concentration).

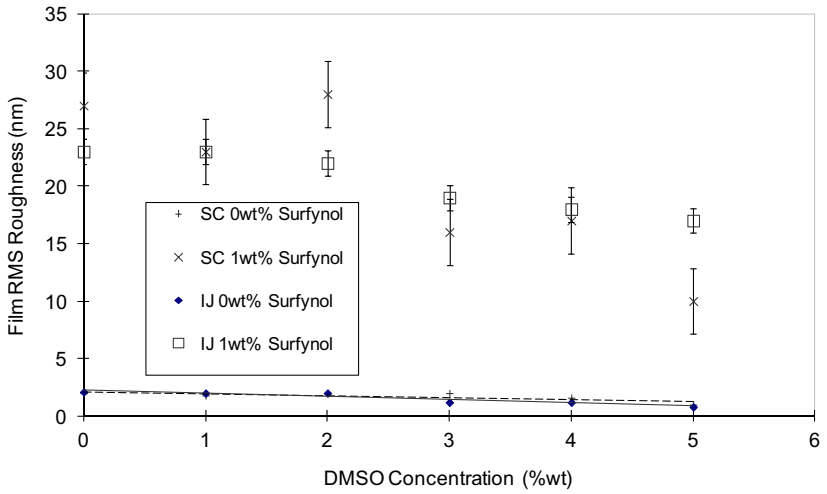

Fig. 8. Surface RMS roughness as a function of dimethyl sulfoxide wt% concentration for 0 and 1 wt% surfactant concentration, and the two alternative film fabrication methods: inkjet printing (IJ) and spin coating (SC).

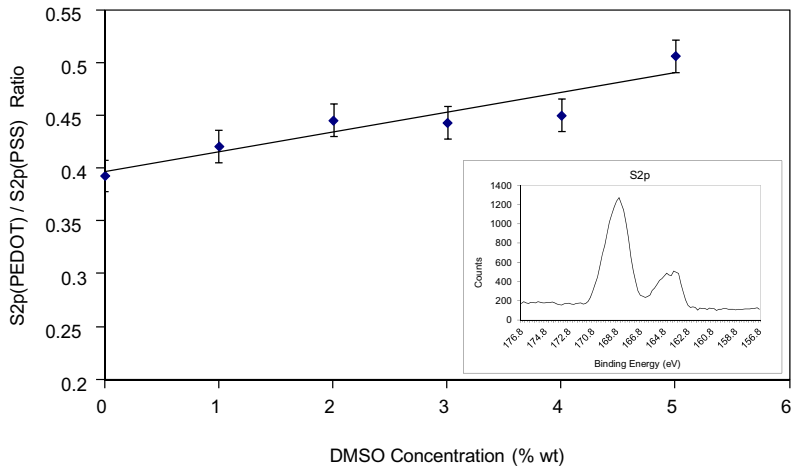

Fig. 9. Relative PEDOT to PSS ratio as measured via the S2p(164 eV) and S2p(169 eV) peak intensities in the XPS spectra of inkjet printed PEDOT:PSS films containing 1 wt% surfactant (Surfynol 2502) and different concentrations of conductivity enhancing co-solvent (DMSO); insert presents the S2p peaks of an inkjet printed sample [4 wt% DMSO, 1 wt% Surfynol].

charge mobility within the sample. This is supported by both XPS and AFM analysis in this study with corresponding reduction of the sheet resistance also demonstrated in Fig. 4 of this study.

4. Conclusions

A host of additives are often required to achieve optimisation in reliability, speed and quality during the inkjet printing process. As inkjet printed electrically conductive films reach mass production, the subtle effects on performance of these additives will play a larger role on the compromise between optimal material properties and optimal processing quality. Within this report it has been demonstrated that inkjet printed thin films offer comparable and even better surface and electrical properties to layers deposited by the more commonly used spin coating technique.

Samples were fabricated by either a custom built inkjet printing unit centred around a MicroFab JetDrive dispensing device or spin cast at 3000 rpm onto microslide substrates. DMSO was the co-solvent investigated in this study and Surfynol 2502 was used optionally as a surfactant which lowered the surface tension of PEDOT:PSS solution, a critical parameter for many inkjet printers; this becomes particularly important when DMSO is added, which resulted in some increase of the surface tension from 60 to 70 mN/m in the absence of surfactant, reaching the upper working limit of many inkjet printers. Surface analysis of the fabricated films was performed as a function of co-solvent concentration, with and without the addition of surfactant, on a Veeco Multimode AFM unit with NanoScope III controller. This was complemented by surface XPS analysis on a ThermoFisher Scientific Theta Probe spectrometer. Electrical characterisation was per-

formed on an Ametek, Princeton Applied Research, 'VersaSTAT MC' twin channel potentiostat/galvanostat, whilst film thickness was recorded using a Veeco Instruments Dektak 8 stylus profilometer.

It has been shown that varying the substrate temperature in inkjet printing results in different profiles of the printed drop, with higher substrate temperatures resulting in smaller printed droplets of cup shape, whereas a substrate temperature of 30 °C yielded a smooth, flat, well spread, printed drop. While there may be applications where printed "cup"-shaped droplets might be useful, for example when a large surface area is desired, in this study the substrate temperature was maintained at about 30 °C and flat drops were printed with 20% overlap. In the course of this work, it has been demonstrated that the inclusion of a surfactant, dictated by the working parameters of most inkjet printing units, generates a considerable increase (by an order of magnitude) in surface roughness for both inkjet and spin coated films. Interestingly, the addition of the surfactant has little effect on the co-solvent-induced conductivity increase, with both spin coated and inkjet printed films demonstrating similar sheet resistances as a function of surfactant concentration. We have shown that the micro-level roughness of inkjet printed films is comparable to those formed by spin coating, where both processes generate an inverse linear correlation between conduction enhancing co-solvent concentration and film RMS roughness due to PEDOT grains (in the cases of 0% Surfynol). AFM surface characterisation also showed coarsening of PEDOT grains when DMSO co-solvent was added while XPS analysis demonstrated a linear increase in the surface PEDOT to PSS ratio against DMSO concentration: the results from both characterisation techniques support the theory that the high dielectric constant of DMSO reduces the electrostatic interaction between the PEDOT polymer and the counter-ion containing PSS resulting in the coarsening of PEDOT domains. Such microstructural effects result in an increase of surface conductivity of the PEDOT:PSS films as the concentration of DMSO is increased, due to the larger PEDOT domains, which are electrically conductive, and reduction of the number of "hops" of the charge carriers over the insulating PSS gaps. Furthermore, inkjet printed films demonstrated higher surface conductivity than spin coated films with equally high concentration of DMSO, attributed to the fact that the inkjet printed films displayed coarser morphology of PEDOT grains than the spin coated films. On the other hand, addition of 1% Surfynol surfactant creates micro-wide features in the film's topography leading to a large increase of surface RMS roughness which, however, does not disadvantage the sheet conductivity of the film due to the fact that it has no effect on the PEDOT grains and their interaction with the surrounding PSS shell.

Acknowledgments

This research was supported by the Innovative Electronics Manufacturing Research Council (IeMRC). Special thanks must go to Dr. Steve Hinder and Simon Ng for all the help with XPS surveys as well as Dr. Andy Smith for guidance on the Hall Probe.

References

[1] W.H. Kim, A.J. Makinen, N. Nikolov, R. Shashidhar, H. Kim, Z.H. Kafafi, Molecular organic light-emitting diodes using highly conducting polymers as anodes, Applied Physics Letters 80 (2002) 3844–3846.
[2] M.A. Lopez, J.C. Sanchez, M. Estrada, Characterization of PEDOT:PSS dilutions for inkjet printing applied to OLED fabrication, 7th International Caribbean Conference on Devices, Circuits and Systems (2008) 165–168.
[3] S.H. Lee, J.Y. Hwang, K. Kang, H. Kang, Fabrication of organic light emitting display using inkjet printing technology, International Symposium on Optomechatronic Technologies (2009) 71–76.
[4] A. Ali, A. Rahman, K.H. Choi, B.S. Yang, D.S. Kim, Interface attachability analysis of printed patterns through electrostatic inkjet system, in: P.J. da Silva Bartolo, M.A. Jorge, F. da Conceicao Batista, H.A. Almeida, J.M. Matias, J.C. Vasco, J.B. Gaspar, M.A. Correia, N.C. Andre, N.F. Alves, P.P. Novo, P.G. Martinho, R.A. Carvalho (Eds.), Innovative Developments in Design and Manufacturing, Taylor & Francis, London, 2010, pp. 377–380.
[5] V.J. Shah, D.B. Wallace, Low-cost Solar Cell Fabrication by Drop-on-Demand Ink-jet Printing, IMAPS 37th (November 14–18, 2004).
[6] M.H. Yun, G.H. Kim, C. Yang, J.Y. Kim, Towards optimization of P3HT:bisPCBM composites for highly efficient polymer solar cells, Journal of Materials Chemistry 20 (2010) 7710–7714.
[7] H.Z. Yu, J.B. Peng, Annealing treatment effect on photoelectric properties of P3HT:PCBM blend system, Acta Physico-Chimica Sinica 24 (2008) 905–908.
[8] J.W. Jung, W.H. Jo, Annealing-free high efficiency and large area polymer solar cells fabricated by a roller painting process, Advanced Functional Materials 20 (2010) 2355–2363.
[9] S.Y.Y. Leung, D.C.C. Lam, Geometric and compaction dependence of printed polymer-based RFID tag antenna performance, 2007 International Conference on Electronic Materials and Packaging (2007) 166–172.
[10] A.Y. Natori, A.M.F. Frasson, A.M. Ceschin. Organic conducting films fabricated with ink jet printing technology and possible application in electric-field probes. in Microwave and Optoelectronics Conference, IMOC 2003. Proceedings of the 2003 SBMO/IEEE MTT-S International (2003).
[11] Y. Shi, J. Liu, Y. Yang, Device performance and polymer morphology in polymer light emitting diodes: the control of thin film morphology and device quantum efficiency, Journal of Applied Physics 87 (2000) 4254–4263.
[12] S.H. Eom, H. Park, S.H. Mujawar, S.C. Yoon, S.S. Kim, S.I. Na, S.J. Kang, D. Khim, D.Y. Kim, S.H. Lee, High efficiency polymer solar cells via sequential inkjet-printing of PEDOT:PSS and P3HT:PCBM inks with additives, Organic Electronics 11 (2010) 1516–1522.
[13] J. Jung, D. Kim, J. Lim, C. Lee, S.C. Yoon, Highly efficient inkjet-printed organic photovoltaic cells, Japanese Journal of Applied Physics 49 (2010) 5.
[14] H. Do, M. Reinhard, H. Vogeler, A. Puetz, M.F.G. Klein, W. Schabel, A. Colsmann, U. Lemmer, Polymeric anodes from PEDOT:PSS for 3.5% efficient organic solar cells, Thin Solid Films 517 (2009) 5900–5902.
[15] H. Mu, W. Li, R. Jones, A. Steckl, D. Klotzkin, A comparative study of electrode effects on the electrical and luminescent characteristics of Alq3/TPD OLED: improvements due to conductive polymer (PEDOT) anode, Journal of Luminescence 126 (2007) 225–229.
[16] B. Ballarin, A. Fraleoni-Morgera, D. Frascaro, S. Marazzita, C. Piana, L. Setti, Thermal inkjet microdeposition of PEDOT:PSS on ITO-coated glass and characterization of the obtained film, Synthetic Metals 146 (2004) 201–205.
[17] H. Sirringhaus, T. Kawase, R.H. Friend, T. Shimoda, M. Inbasekaran, W. Wu, E.P. Woo, High-resolution inkjet printing of all-polymer transistor circuits, Science 290 (2000) 2123–2126.
[18] S.H. Eom, S. Senthilarasu, P. Uthirakumar, S.C. Yoon, J. Lim, C. Lee, H.S. Lim, J. Lee, S.-H. Lee, Polymer solar cells based on inkjet-printed PEDOT:PSS layer, Organic Electronics 10 (2009) 536–542.
[19] K.X. Steirer, J.J. Berry, M.O. Reese, M.F.A.M. Van Hest, A. Miedaner, M.W. Liberatore, R.T. Collins, D.S. Ginley, Ultrasonically sprayed and inkjet printed thin film electrodes for organic solar cells, Thin Solid Films 517 (2009) 2781–2786.
[20] A.U. Chen, O.A. Basaran, A new method for significantly reducing drop radius, Physics of Fluids 14 (2002) L1–L4.
[21] A.U. Chen, O.A. Basaran, Method and apparatus for producing drops using a drop-on-demand dispenser, US Patent, 6513,894 B1 (February 2003).
[22] S.K.M. Jonsson, J. Birgerson, X. Crispin, G. Greczynski, W. Osikowicz, A.W.D. van der Gon, W.R. Salaneck, M. Fahlman, The effects of

solvents on the morphology and sheet resistance in poly (3,4-ethylenedioxythiophene)–polystyrenesulfonic acid (PEDOT–PSS) films, Synthetic Metals 139 (2003) 1–10.
[23] B.Y. Ouyang, C.W. Chi, F.C. Chen, Q.F. Xi, Y. Yang, High-conductivity poly (3,4-ethylenedioxythiophene):poly(styrene sulfonate) film and its application in polymer optoelectronic devices, Advanced Functional Materials 15 (2005) 203–208.
[24] A.M. Nardes, R.A.J. Janssen, M. Kemerink, A morphological model for the solvent-enhanced conductivity of PEDOT:PSS thin films, Advanced Functional Materials 18 (2008) 865–871.
[25] A.M. Nardes, M. Kemerink, M.M. De Kok, E. Vinken, K. Maturova, R.A.J. Janssen, Conductivity, work function, and environmental stability of PEDOT:PSS thin films treated with sorbitol, Organic Electronics 9 (2008) 727–734.
[26] A.M. Nardes, M. Kemerink, R.A.J. Janssen, Anisotropic hopping conduction in spin-coated PEDOT:PSS thin films, Physical Review B 76 (2007) 085208-1–085208-7.
[27] A.M. Nardes, M. Kemerink, R.A.J. Janssen, J.A.M. Bastiaansen, N.M.M. Kiggen, B.M.W. Langeveld, A.J.J.M. Van Breemen, M.M. de Kok, Microscopic understanding of the anisotropic conductivity of PEDOT:PSS thin films, Advanced Materials 19 (2007) 1196–1200.
[28] R.D. Deegan, O. Bakajin, T.F. Dupont, G. Huber, S.R. Nagel, T.A. Witten, Contact line deposits in an evaporating drop, Physical Review E 62 (2000) 756–765.
[29] R.D. Deegan, Pattern formation in drying drops, Physical Review E 61 (2000) 475–485.
[30] B. Zhmud, Dynamic aspects of ink-paper interactions in relation to inkjet printing, Pira International Conference: Ink on Paper (2003) Brussels, Belgium.
[31] J.-W. Song, Inkjet printing of single-walled carbon nanotubes and electrical characterization of the line pattern, Nanotechnology 19 (2008) 095702.
[32] J.Y. Kim, J.H. Jung, D.E. Lee, J. Joo, Enhancement of electrical conductivity of poly(3,4-ethylenedioxythiophene)/poly(4-styrenesulfonate) by a change of solvents, Synthetic Metals 126 (2002) 311–316.
[33] E. Montibon, L. Jarnstrom, M. Lestelius, Characterisation of poly(3,4-ethylenedioxythiophene)/poly(styrene sulfonate) (PEDOT:PSS) adsorption on cellulosic materials, Cellulose 16 (2009) 807–815.
[34] S. Ashizawa, R. Horikawa, H. Okuzaki, Effects of solvent on carrier transport in poly(3,4-ethylenedioxythiophene)/poly(4-styrenesulfonate), Synthetic Metals 153 (2005) 5–8.